Proc. Natl. Acad. Sci. USA
Vol. 93, pp. 4229–4234, April 1996
Neurobiology

Glycoprotein 330/megalin: Probable role in receptor-mediated transport of apolipoprotein J alone and in a complex with Alzheimer disease amyloid β at the blood–brain and blood–cerebrospinal fluid barriers

(binding–transport)

BERISLAV V. ZLOKOVIC*†, CYNTHIA L. MARTEL*, ETSURO MATSUBARA‡, J. GORDON MCCOMB*, GANG ZHENG§, ROBERT T. MCCLUSKEY§, BLAS FRANGIONE‡, AND JORGE GHISO‡

*Department of Neurological Surgery and Division of Neurosurgery, Childrens Hospital, and University of Southern California School of Medicine, Los Angeles, CA 90033; ‡Department of Pathology, New York University Medical Center, New York, NY 10016; and §Department of Pathology, Harvard Medical School, Boston, MA 02129

Communicated by Marilyn Gist Farquhar, University of California, San Diego, La Jolla, CA, December 28, 1995 (received for review November 5, 1995)

ABSTRACT **A soluble form of Alzheimer disease amyloid β-protein (sAβ) is transported in the blood and cerebrospinal fluid mainly complexed with apolipoprotein J (apoJ). Using a well-characterized *in situ* perfused guinea pig brain model, we recently obtained preliminary evidence that apoJ facilitates transport of $sA\beta_{1-40}$–apoJ complexes across the blood–brain barrier and the blood–cerebrospinal fluid barrier, but the mechanisms remain poorly understood. In the present study, we examined the transport process in greater detail and investigated the possible role of glycoprotein 330 (gp330)/megalin, a receptor for multiple ligands, including apoJ. High-affinity transport systems with a K_m of 0.2 and 0.5 nM were demonstrated for apoJ at the blood–brain barrier and the choroid epithelium *in vivo*, suggesting a specific receptor-mediated mechanism. The $sA\beta_{1-40}$–apoJ complex shared the same transport mechanism and exhibited 2.4- to 10.2-fold higher affinity than apoJ itself. Binding to microvessels, transport into brain parenchyma, and choroidal uptake of both apoJ and $sA\beta_{1-40}$–apoJ complexes were markedly inhibited (74–99%) in the presence of a monoclonal antibody to gp330/megalin and were virtually abolished by perfusion with the receptor-associated protein, which blocks binding of all known ligands to gp330. Western blot analysis of cerebral microvessels with the monoclonal antibody to gp330 revealed a protein with a mass identical to that in extracts of kidney membranes enriched with gp330/megalin, but in much lower concentration. The findings suggest that gp330/megalin mediates cellular uptake and transport of apoJ and $sA\beta_{1-40}$–apoJ complex at the cerebral vascular endothelium and choroid epithelium.**

The principal constituent of Alzheimer disease amyloid deposits, amyloid β (Aβ) peptide (39–44 residues), has been recently found in a soluble form (sAβ) in plasma, cerebrospinal fluid, and cell culture supernatants (1). sAβ in biological fluids contains mainly peptide 1–40, which is similar to Aβ isolated from cerebrovascular amyloid, whereas a small portion of sAβ corresponds to $A\beta_{1-42}$, which is the predominant component of parenchymal Alzheimer disease deposits (1–4). The discovery of circulating sAβ supports the hypothesis that Alzheimer disease and systemic amyloidoses may have unifying features (1). Recent findings from our laboratory, and others, have demonstrated that a synthetic peptide homologous to $A\beta_{1-40}$ is avidly taken up from the circulation by guinea pig brain capillaries (5) and is transported as intact peptide across the mice blood–brain barrier (BBB) (6).

The publication costs of this article were defrayed in part by page charge payment. This article must therefore be hereby marked "*advertisement*" in accordance with 18 U.S.C. §1734 solely to indicate this fact.

It is uncertain whether sAβ is the immediate precursor of Aβ, and if so, how the transition from soluble to filamentous form is brought about (7). Several lines of evidence suggest that apolipoprotein E (apoE) and apolipoprotein J (apoJ), also known as clusterin (8, 9), may be involved in the regulation of amyloid formation. They both bind sAβ/Aβ *in vivo* and *in vitro* (10, 11). There is evidence that apoE may modulate β-pleated conformation of Aβ (1). In addition, the inheritance of apoE4 allele has been identified as a risk factor for late-onset Alzheimer disease (11). ApoJ has been shown to be the major carrier protein of sAβ in the cerebral spinal fluid and plasma (7). *In vitro* studies have demonstrated that the $sA\beta_{1-40}$–apoJ complex cannot be dissociated by apoE2, apoE3, apoE4, and/or other amyloid-associated proteins such as α_1-antichymotrypsin, vitronectin, and transthyretin at their physiologic plasma concentrations (12).

Using a well-established guinea pig brain perfusion model (13), we have recently obtained evidence that apoJ and $sA\beta_{1-40}$–apoJ complexes are taken up at the BBB *in vivo* by a high-affinity transport mechanism typical of receptor-mediated transcytosis (14, 15). However, the actual receptor remained unidentified. In the present study we have further characterized the transport mechanism for $sA\beta_{1-40}$–apoJ complexes and free apoJ at the BBB and blood–cerebrospinal fluid barrier.

In particular, we examined the possible role of the receptor glycoprotein 330 (gp330)/megalin (16) in the transport process. gp330/megalin, a member of the low density lipoprotein (LDL) receptor family (17), has been shown to bind multiple ligands *in vitro*, including apoJ, which exhibits an unusually high affinity (18). The binding of ligands to gp330/megalin can be inhibited by a 39- to 44-kDa protein called the receptor-associated protein (RAP). This protein forms a complex with gp330 shortly after biosynthesis and remains largely confined to the rough endoplasmic reticulum (19). Although RAP is not normally secreted, it can be produced in soluble form as a fusion protein, which can be used to block binding of ligands to gp330 (or other members of the LDL receptor family) *in vitro* or *in vivo* (20, 21). Little is known about functions of megalin *in vivo* (22), but its role as a drug receptor has been recently demonstrated (23). In the present study we investigated the role of gp330 on brain uptake of apoJ and the $sA\beta_{1-40}$–apoJ complex by pre- and coperfusing the brain with RAP or with a monoclonal antibody to gp330.

Abbreviations: Aβ, amyloid β; sAβ, soluble Aβ; apoE, apolipoprotein E; gp330, glycoprotein 330; BBB, blood–brain barrier; LDL, low density lipoprotein; RAP, receptor-associated protein; GST, glutathione *S*-transferase; PS, permeability surface product; apoJ, apolipoprotein J.

†To whom reprint requests should be addressed.

MATERIALS AND METHODS

Animals. Guinea pigs (Hartley strain) of either sex and 250–300 g body weight were obtained from Charles River Breeding Laboratories. All animals were kept a minimum of 3 days under standard housing conditions and feeding schedules before the experiments.

Vascular Brain Perfusion. Animals were anesthetized intramuscularly with 6 xylazine at mg/kg (Rompun; Mobay Chemical) and ketamine at 30 mg/kg (Ketacet; Aveco, Fort Dodge, IA) before surgical exposure of the neck vessels. Details of the vascular brain perfusion technique have been described (13, 14).

Synthetic Peptide and Proteins. Peptide DAEFRHDSGYEVHHQKLVFFAEDVGSNKGAIIGLMVGGVV ($sA\beta_{1-40}$), which corresponds to residues 672–711 of βPP770, was synthesized at the W. M. Keck Facility at Yale University using solid phase *N-tert*-butyloxycarbonyl chemistry. The final product was lyophilized and characterized by analytical reverse-phase HPLC, amino acid analysis, laser desorption spectrometry, and CD. The $A\beta_{1-40}$ used in this study (batch JK420GHI) had the following secondary structure deduced from CD: α-helix = 0%; β-sheet = 27.7%; random coil = 71.7%; and β-turn = 0.6%. Other authors have reported studies in rats with $A\beta_{1-40}$ obtained from Bachem (24), with different secondary structure (β-sheet, ≈80%), so their data are not directly comparable, and may not reflect the BBB transport of sAβ well. Human apoJ was from Quidel (San Diego). Protein purity was corroborated by SDS/PAGE and N-terminal sequence analysis.

Anti-gp330 Antibody and RAP. A previously characterized anti-gp330 monoclonal antibody, 1H2, was used (25, 26). 1H2 was obtained by immunization of mice with immunoaffinity-purified gp330 and by screening with ELISA for monoclonal antibody reactive with immunoaffinity-purified rat gp330 (25). 1H2 reacts with gp330 obtained by affinity purification on a column containing RAP (27). In the present study, we confirmed that 1H2 reacts with guinea pig gp330 by its ability to stain brush-border regions of renal proximal tubules in frozen sections and by Western blot analysis with renal extracts. A RAP–glutathione *S*-transferase (GST) fusion protein was prepared as described (28). To detect reactivity of the fusion protein with guinea pig gp330, frozen sections of guinea pig kidney were incubated with RAP–GST, followed by staining for GST. Intense staining of proximal tubule brush borders was seen, indicating that RAP–GST had combined with gp330. Incubation of sections with GST alone did not produce staining.

Complex Formation and Characterization. The complexes composed of $sA\beta_{1-40}$ and apoJ were formed in phosphate-buffered saline (20 μM Na phosphate 150 μM NaCl, pH 7.4) by incubating the purified components at a 15:1 ($sA\beta_{1-40}$ to apoJ) molar ratio for 3 hr at 37°C. Under these conditions, all available apoJ is complexed to $sA\beta_{1-40}$. Purification of the complex was achieved by means of a modified reverse-phase HPLC using a Vydac (The Separations Group) C_4 microbore column (214 TP 52; 0.21 × 25 cm) and a 25-min 3–70% linear gradient of acetonitrile in water (pH 3.1 adjusted with trifluoroacetic acid) at a flow rate of 0.2 ml/min. Further identification was achieved by amino acid sequence and Western blot analysis.

Radioiodination. Proteins were labeled with $Na^{125}I$ [13.7 mCi/μg (1 Ci = 37 GBg); Amersham] using Iodobeads (Pierce) following the manufacturer's instructions. The specific activities were 5.3 and 6.9 μCi/μg for ^{125}I-labeled $sA\beta_{1-40}$ and apoJ, respectively. Labeling of the complex was always on apoJ. In all cases, radioactivity was 98% trichloroacetic acid-precipitable. Changes in the secondary structure due to the radioiodination procedure were evaluated by CD measurements.

Solid-phase Binding Studies and Competitive Inhibition Assay. The influence of radioiodination on $sA\beta_{1-40}$–apoJ was studied by ELISA using $sA\beta_{1-40}$ and purified native and ^{125}I-labeled human apoJ. Binding studies and competitive inhibition assays were done essentially as described (12).

Brain Uptake Measurements. Radioiodinated $sA\beta_{1-40}$, apoJ, and $sA\beta_{1-40}$–apoJ complexes were introduced separately into the perfusion circuit by a Harvard Apparatus slow-drive syringe pump at a rate of 0.2 ml/min within periods from 1 to 10 min. [^{14}C]Sucrose was used as a standard cerebrovascular space marker. The uptake of ^{125}I-labeled apoJ and ^{125}I-labeled $sA\beta_{1-40}$–apoJ complexes was studied in the presence of unlabeled proteins, the anti-gp330 antibody, and RAP. Unlabeled proteins, anti-gp330 antibody, and RAP were preinfused into the brain 5 min before perfusion of ^{125}I-labeled ligand, and then for an additional 10 min simultaneously with labeled ligand. The perfusion was terminated by severing the right common carotid artery, and guinea pigs were then decapitated. The ipsilateral cerebral cortex was quickly removed from the skull, arachnoid membranes were peeled away, and the choroid plexus was separated by dissection. The ^{125}I and ^{14}C radioactivities in homogenized tissues were determined in a Beckman 4000 gamma counter and Beckman LS-7500 liquid scintillation spectrometer, respectively.

Binding to Microvessels and Transendothelial Transport. In some experiments, after a 10-min perfusion, the brain tissue was subjected to a capillary depletion procedure, and microvessels were separated from the perfused brain, as reported (14). The microvessel preparation contained ≈95% capillaries and ≈5% small arterioles and venules, and the capillary-depleted brain was essentially free of blood vessels, as we reported (29).

Calculations. Volume of distribution (V_D) for iodinated proteins and sucrose in the brain, microvessels, capillary-depleted brain, and choroid plexus was calculated as follows (13, 14).

$$V_D = C_{IN}/C_{PL}, \quad [1]$$

where C_{IN} and C_{PL} are dpm or cpm/g of tissue, and dpm or cpm/ml of perfusate, for ^{125}I or ^{14}C radioactivities. The unidirectional transport rate constant, K_{IN}, for test tracers was calculated using the equation

$$K_{IN} = [V_D(\text{test tracer}) - V_D(\text{sucrose})]/T \quad [2]$$

as reported (13, 14), where T is the perfusion time. The cerebrovascular permeability coefficient (P) × capillary surface area (S) product (PS) is the same as the K_{IN} value if $PS \ll$ cerebral blood flow (14), a condition satisfied by substances used in this study. When ^{125}I-labeled apoJ was studied with various concentrations of unlabeled apoJ, kinetic parameters were calculated as follows (13, 14):

$$K_{IN} = V_{max}/(K_m + C_{PL}). \quad [3]$$

The inhibitory constant, K_i, for the inhibition of ^{125}I-labeled apoJ uptake by a complex was determined by the use of a "velocity ratio," as we reported (14). Because blood flow ≫ PS, the influx $J_{IN} = PS \cdot C_{PL}$, as reported (13).

Western Blot Analysis. Choroid plexus, cerebral microvessel, and capillary-depleted brain homogenates were prepared as we described (29). Extracts from kidney membranes enriched in gp330 were prepared, as reported (27). Proteins (20 μg/lane) were separated on a SDS/10% PAGE minigel, transferred to nitrocellulose paper at 4°C, the membranes blocked in 5% nonfat milk in Tris/borate/saline at 4°C overnight, and incubated at 37°C for 3 hr with the 1H2 anti-gp330 antibody. Goat anti-mouse IgG was a secondary antibody. The enhanced chemiluminescence detection system (Amersham) was used to detect proteins.

RESULTS

Fig. 1*A* illustrates significant time-dependent uptake of ^{125}I-labeled apoJ by the cerebral cortex in guinea pigs during 10 min of brain perfusion. Low uptake of [^{14}C]sucrose is also shown. Fig. 1*B* shows that the *PS* value for ^{125}I-labeled apoJ depends on the concentration of unlabeled apolipoprotein in the plasma perfusate.

Almost identical molar ellipticity plots were obtained for native and ^{125}I-labeled apoJ, indicating that no significant structural modifications were produced by the incorporation of ^{125}I (Fig. 2*A*). To exclude the possibility that the procedure altered the ability of apoJ to interact with sAβ_{1-40}, solid-phase ELISA experiments at physiologic pH were conducted with both native and radioiodinated apoJ. Analysis of the binding isotherms (Fig. 2*B*) revealed no major differences in the dissociation constant (K_d) between the two forms of apoJ. In addition, the IC_{50} values of labeled and unlabeled apoJ required to inhibit the binding of biotin-labeled apoJ to immobilized sAβ_{1-40} were also comparable (Fig. 2*C*).

Fig. 3 illustrates the HPLC separation of the sAβ_{1-40}–apoJ complex. At pH 2.1, complete complex dissociation was achieved, and two components eluting at 58% (peak A) and 65% (peak B) of acetonitrile were obtained. The retention times were identical to those observed for the purified sAβ_{1-40} (19 min, 58% acetonitrile) and apoJ (23 min, 65% acetonitrile). Complex isolation was achieved at pH 3.1; an extra peak showing an intermediate retention time (21.5 min) was obtained at 62% acetonitrile (peak C). Amino-terminal sequence analysis of peak C rendered three equimolar sequences DQTVSDNELQ, SLMPFSPYEP, and DAEFRHDSGY, corresponding to the first 10 residues of the apoJ α-chain, apoJ β-chain, and sAβ_{1-40}, respectively. In a native non-SDS gel, the complex exhibited a M_r ≈85,000 (peak C), and it was recognized by both anti-Aβ and anti-apoJ antibodies in Western blot analysis (Fig. 3, arrowheads), whereas peaks A and B were reactive only with anti-Aβ and anti-apoJ antibodies, respectively.

Table 1 illustrates that the *PS* value for sAβ_{1-40}–apoJ complex is 37.5-fold higher than for sucrose and is 4.5-fold and 2.4-fold higher than for sAβ_{1-40} and apoJ, respectively. There was no correlation between the *PS* values of tested peptides/proteins, either with their partition coefficient or the reciprocal value of the square root of the molecular weight. Michaelis–Menten analysis of data given in Fig. 1*B* (Eq. **3**), as well as of the choroid plexus data (data not shown), revealed the presence of specific transport systems for apoJ with remarkably high affinities, between 0.2 and 0.5 nM (Table 2). Transport of apoJ was significantly inhibited by the sAβ_{1-40}–apoJ complex,

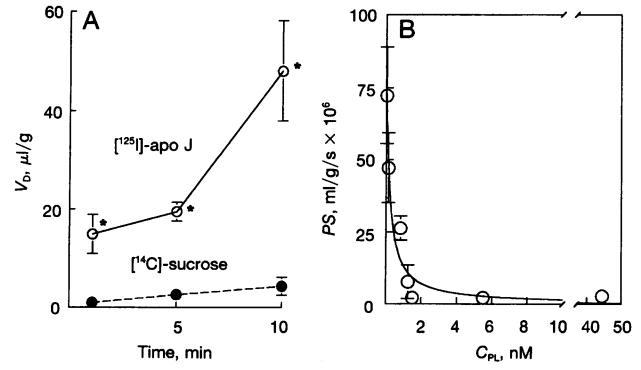

FIG. 1. Blood-to-brain uptake of apoJ in perfused guinea pig brain. (*A*) Kinetics of entry of radiolabeled apoJ (0.02 nM) and sucrose into the cerebral cortex plotted against the perfusion time. V_D, volume at distribution (*B*) *PS* for ^{125}I-labeled apoJ (0.02 nM) is plotted against concentration of unlabeled apoJ in the perfusate C_{PL}. Each point represents mean ± SE; n = 3–7; *, $P < 0.01$ by ANOVA.

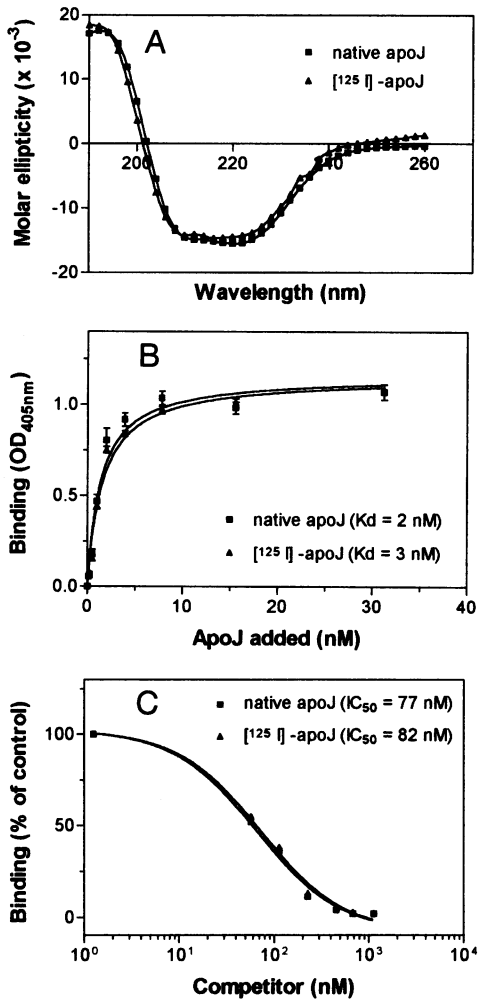

FIG. 2. (*A*) CD studies. (*B* and *C*) *In vitro* binding isotherms to immobilized sAβ_{1-40} (*B*), and competitive inhibition of biotin-labeled apoJ to immobilized sAβ_{1-40} (*C*) of native and ^{125}I-labeled apoJ.

and the analysis of the K_i constants at equimolar concentrations indicated that the complex has 2.4 and 10.2 times higher affinity for the BBB and choroid plexus transport, respectively, than the apoJ itself.

Transport into brain parenchyma (Fig. 4*A*), sequestration by brain capillaries (Fig. 4*B*), and uptake by the choroid plexus (Fig. 4*C*) of ^{125}I-labeled apoJ were strongly inhibited (74–99%) by the anti-gp330 antibody 1H2 (5.4 nM). In the presence of 20 nM RAP (in the form of RAP–GST fusion protein), the uptake of apoJ was completely abolished, while GST was without effect (data not shown). Fig. 5 illustrates that compartmental uptake of ^{125}I-labeled sAβ_{1-40}–apoJ complex was significantly inhibited (75–98%) by the anti-gp330 antibody

Table 1. Cerebrovascular permeability to iodinated sAβ_{1-40}, apoJ, and sAβ_{1-40}–apoJ

Peptide/protein	*PS*, ml/g per s × 10^6	n	*PC*	$1/\sqrt{M}$
sAβ_{1-40}	44.7 ± 5.3	19	0.0350	0.0151
apoJ	72.3 ± 16.6	8	0.0964	0.0035
sAβ_{1-40}–apoJ	172.7 ± 37.5*	7	0.0459	0.0034

Data are expressed as means ± SE; n is the number of perfused brains. *PS* values for peptide/protein are significantly higher than for sucrose (*PS* = 4.6 ± 1.3, n = 12). *PC*, partition coefficient in octanol/Ringer's solution.

*$P < 0.01$ for sAβ_{1-40}–apoJ vs. sAβ_{1-40} and for sAβ_{1-40}–apoJ vs. apoJ by ANOVA with Newman–Keuls multiple comparison test.

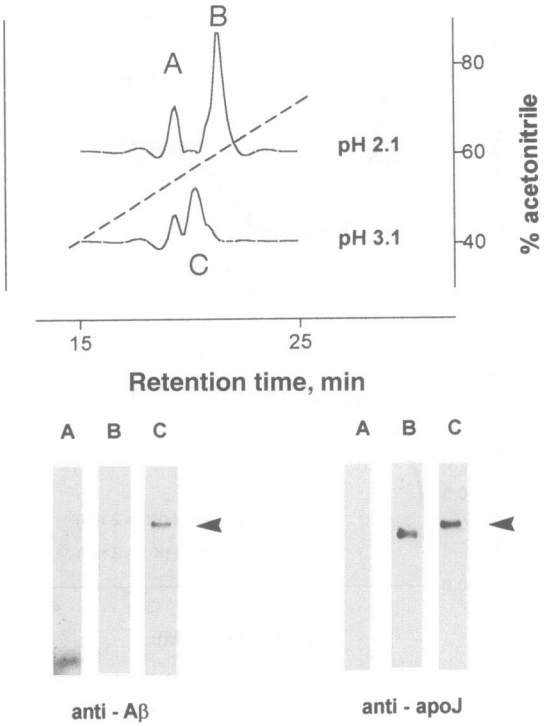

FIG. 3. (*Upper*) HPLC separation of $sA\beta_{1-40}$–apoJ complex. Peaks A and B correspond to the retention times of $sA\beta_{1-40}$ and apoJ at pH 2.1; isolation of the complex was achieved at pH 3.1 (peak C). (*Lower*) Western blot analysis of peaks A, B, and C in native non-SDS gel with anti-Aβ (*Left*) and anti-apoJ (*Right*) antibodies. Arrowheads indicate the complex.

and that RAP abolished the uptake of complexes in brain compartments and produced 74% inhibition in the plexus. At apoJ concentrations as high as 9 nM, the uptake of complexes was abolished in capillary-depleted brain and microvessels and inhibited by 75% in the plexus. In contrast, 9 nM of unlabeled $sA\beta_{1-40}$ was without effect on uptake of complexes.

Western blot analysis (Fig. 6*A*) of microvessels and choroid plexus with the monoclonal antibody to gp330 revealed a protein with a mass similar to that found in extracts of kidney membranes enriched with gp330/megalin, but the band was considerably less intense. The gp330 signal was absent from the capillary-depleted brain. Reverse-phase HPLC of the soluble extracts obtained after homogenization of a brain perfused for 10 min with ^{125}I-labeled apoJ revealed the presence of a single radioactive peak exhibiting the same retention time as the native apoJ (data not shown). As indicated in Fig. 6*B*, SDS/PAGE analysis of the radioactive peak performed under nonreducing conditions showed a major 80-kDa component and a minor 160-kDa band, corresponding to monomeric and dimeric forms of apoJ, respectively. Under reducing conditions, as expected, a major 40-kDa band was observed, consistent with the disulfide-bonded heterodimeric structure of the molecule (8). The apoJ identity of the radioactive components shown in Fig. 6*B* was confirmed with Western blot analysis using anti-apoJ antibodies and enhanced chemiluminescence as a detection system (data not shown).

Table 2. Kinetic parameters of apoJ transport and inhibition by complex

	K_m, nM	V_{max}, fmol/min per g	K_i, nM	K_i/K_m
Brain	0.19 ± 0.02	0.93 ± 0.09		
$sA\beta_{1-40}$–apoJ			0.09 ± 0.02	0.46
apoJ			0.21 ± 0.02	1.11
Choroid plexus	0.51 ± 0.07	16.7 ± 2.05		
$sA\beta_{1-40}$–apoJ			0.12 ± 0.05	0.23
apoJ			1.20 ± 0.16	2.35

Data are means ± SE based on 18–22 perfused brains. K_i for the complex and apoJ were estimated at 0.1 nM.

DISCUSSION

This study has demonstrated remarkable cerebrovascular permeability to circulating apoJ and $sA\beta_{1-40}$–apoJ complexes, and significant uptake of these ligands by the choroid plexus. The cerebrovascular permeability, expressed as PS, for the $sA\beta_{1-40}$–apoJ complex and free apoJ were among the highest ever recorded for proteins at the BBB (Table 1; Figs. 1*A*, 4*A*, and 5*A*) (14). The *PS* value for $sA\beta_{1-40}$–apoJ was 9- to 14-fold higher than for insulin, a peptide considered to have significant cerebrovascular permeability mediated by endothelial insulin receptor (30), which also transports circulating anti-insulin receptor monoclonal antibody (31). In comparison with transferrin and nerve growth factor, the *PS* value of the complex was 45- to 99-fold higher (depending on brain region) (30). The *PS* value of OX26 antibody to transferrin BBB receptor, which mediates BBB transport of OX26–$A\beta_{1-40}$ complex (24), was 17-fold lower than that of $sA\beta_{1-40}$–apoJ complex. When compared to vascular markers albumin and dextran (M_r, 70,000), the *PS* value for the complex was 1350- to 3600-fold higher (30). A significant amount of apoJ and $sA\beta_{1-40}$–apoJ complex remained associated with microvessels (Figs. 4 and 5).

As indicated in Table 1, lipophilicity and passive diffusion are probably not the primary factors responsible for the difference in permeability between the three ligands (14). The present study confirms that apoJ transport, presumably initiated at the luminal side of the BBB and the basolateral side of the choroid plexus (Fig. 1 and Table 2), is mediated by specific transport systems that exhibit even higher affinity for the complex. The importance of these transport systems under

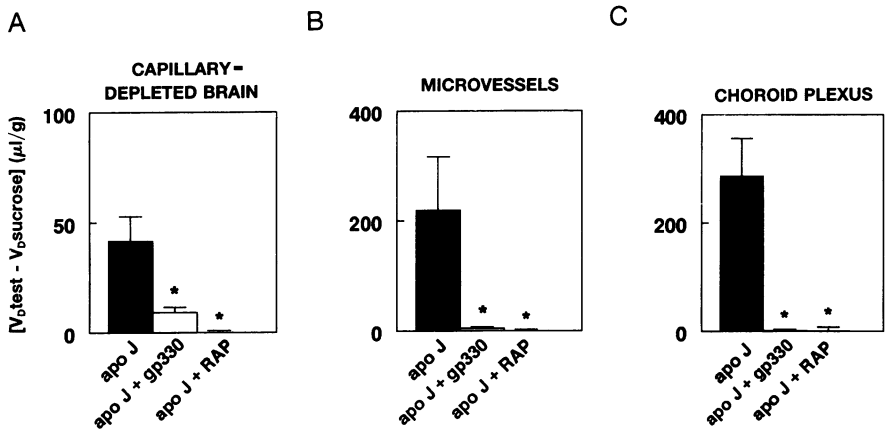

FIG. 4. Compartmental brain distribution of radioiodinated apoJ in the presence of unlabeled anti-gp330 antibodies (5.4 nM) and RAP (20 nM) in capillary-depleted brain (*A*), microvessels (*B*), and choroid plexus (*C*). Values are means ± SE; $n = 5$–8. *, $P < 0.001$ for radiolabeled apoJ in the presence and absence of either anti-gp330 antibodies or RAP by ANOVA. V_D, volume of distribution.

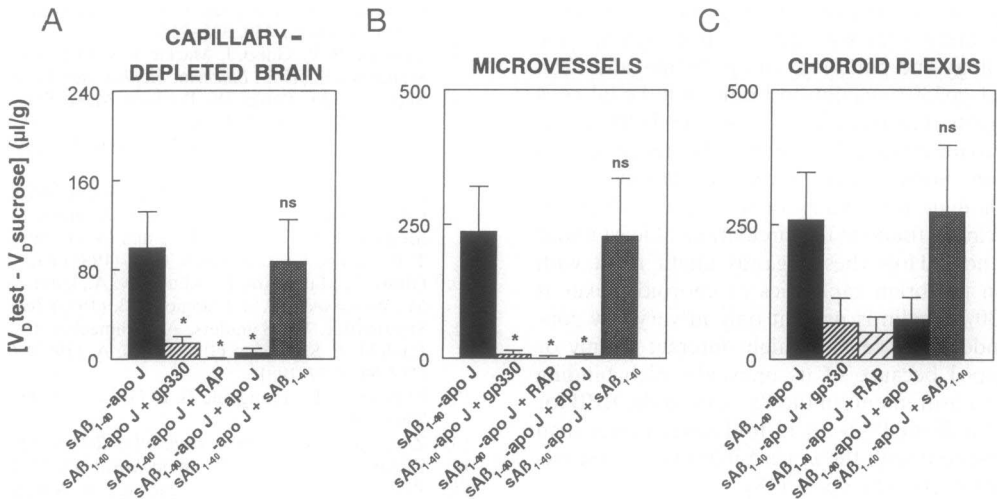

FIG. 5. Compartmental brain distribution of radioiodinated $sA\beta_{1-40}$–apoJ complex in the presence of unlabeled anti-gp330 antibodies (5.4 nM), RAP (20 nM), apoJ (9 nM), and $sA\beta_{1-40}$ (9 nM) in capillary-depleted brain (*A*), microvessels (*B*), and choroid plexus (*C*). Values are means ± SE; $n = 5–8$. *, $P < 0.001$ for radiolabeled $sA\beta_{1-40}$–apoJ in the presence and absence of either anti-gp330 antibodies, RAP, or apoJ, by ANOVA. ns, Nonsignificant for radiolabeled $sA\beta_{1-40}$–apoJ in the presence and absence of $sA\beta_{1-40}$, by ANOVA. V_D, volume of distribution.

physiologic conditions and their possible role in the development of Aβ deposits remain to be elucidated. In plasma, sAβ is mainly complexed with apoJ (10) and incorporated into high density lipoprotein fraction 3 and very high density lipoprotein (32), and apoJ is also predominantly associated with high density lipoprotein (33). The ligands in the present study were tested free of their specific lipoproteins, and the extent to which apoJ or $sA\beta_{1-40}$–apoJ combined with high density lipoprotein is sequestered and transported at the BBB or the choroid plexus is unknown. However, it is known that apolipoproteins can dissociate from lipoproteins *in vivo*, and evidence has been obtained that apoA1 is filtered across the glomerular barrier (34).

The extremely high BBB affinity and transport of $sA\beta_{1-40}$–apoJ and apoJ would argue for the involvement of a specific receptor (14), as in the case of insulin, insulin-like growth factors, transferrin, and vasopressin. The following lines of evidence indicate that gp330/megalin is likely the responsible receptor. (*i*) Binding of $sA\beta_{1-40}$–apoJ and free apoJ to brain capillaries and choroid plexus was strongly inhibited by perfusion with a monoclonal antibody to gp330 and was virtually abolished by perfusion with RAP, a protein known to prevent

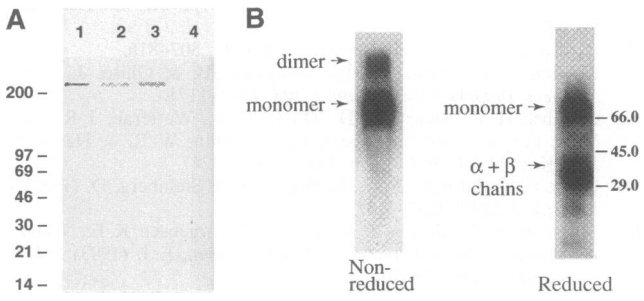

FIG. 6. (*A*) Western blot analysis of proteins (20 μg per lane) from kidney membranes (lane 1), cerebral microvessels (lane 2), choroid plexus (lane 3), and capillary-depleted brain (lane 4). Proteins were separated on a minigel, and the membranes were incubated with 1H2 anti-gp330/megalin (1 μg/ml). (*B*) SDS/PAGE analysis of brain tissue perfused for 10 min with ^{125}I-labeled apoJ. The radioactivity in the brain was eluted as a single peak on HPLC with the same retention time as the apoJ standard (data not shown). Reduced and nonreduced aliquots of the lyophilized sample were subjected to 10% Tris Tricine SDS/PAGE, transferred to a nitrocellulose membrane, and exposed to x-ray film.

binding of ligands to gp330 (21, 27, 35) (Figs. 4 and 5). (*ii*) Furthermore, binding was mediated by apoJ, a high-affinity ligand for gp330, not known to bind to other receptors, including other members of the LDL receptor family (18). (*iii*) Western blot analysis of a brain microvessel preparation with the monoclonal antibody anti-gp330 revealed reactivity with a band identical to that found in kidney membranes enriched in megalin (Fig. 6*A*). The intensity of the gp330/megalin band seen in cerebral microvessels was significantly lower than in kidney, consistent with the interpretation that gp330 is expressed at the BBB at lower levels. Findings of gp330/megalin in choroid plexus confirmed previous results in mouse brain (36).

The failure to detect gp330 on endothelial cells by previous immunocytochemical studies of rat (26, 37), mouse (36), or human brain (38) may reflect a very low concentration on these cells. Thus, certain proteins, such as the angiotensin-converting enzyme, cannot be detected by immunofluoresence on glomerular endothelial cells, although after renal perfusion with anti-angiotensin-converting enzyme antibodies, clumping and patching of complexes occurs on these cells, indicating the antigen (39). Preliminary studies in our laboratory indicated the presence of gp330 mRNA in brain capillaries by a PCR approach (data not shown). Whether gp330/megalin in the brain endothelium is a form of gp330 similar or different to that found in other organs (26, 36, 38) or is an unrecognized receptor (possibly a member of the LDL receptor superfamily) remains to be answered by molecular cloning. Although the LDL receptor itself is expressed on brain capillary endothelium and mediates transport of several ligands and drugs (40), this receptor is not known to bind apoJ.

It is believed that gp330/megalin is a receptor that mediates endocytosis of ligands (16, 37, 41) because of its presence in coated pits and possession of NPXY sequences in the cytoplasmic domain, known to be internalization signals. *In vitro* studies, using immunoassays or cultured cells, have identified a number of ligands in addition to apoJ capable of binding to gp330/megalin, including lipoprotein lipase, apoE-enriched β very low density lipoprotein, tissue-plasminogen activator, plasminogen activators complexed to plasminogen activator inhibitor-1, aprotinin, Ca^{2+}, and lactoferrin (27). Most of the ligands, not including apoJ, also bind to the LDL receptor-related protein, which has been shown to mediate uptake of circulating ligands by the liver (42). However, there is still little direct evidence about functions of gp330/megalin with respect to its physiological ligands in specialized milieus such as the glomerular filtrate, airways, epididymal fluid, thyroid colloid,

and yolk sac fluid (26, 36). The recently suggested role in the uptake of certain drugs (22) has opened an intriguing new chapter in the biology and pathology of gp330/megalin (21).

The presence of gp330/megalin on brain endothelial cells and its role in mediating transport across the BBB would represent a hitherto unsuspected function of this receptor, and one with important implications concerning its physiologic function and pathologic role. Many of the ligands of gp330 identified *in vitro* can be found in the circulation, at least under certain circumstances. How these ligands might react with gp330/megalin on the brain capillaries or choroid plexus is unknown. If gp330/megalin is present only in very low concentrations on endothelial cells, it might interact mainly or exclusively with apoJ because of its unusually high binding affinity (18). Our measurements of the *PS* value at the BBB for apoE3 and apoE4 indicated ≈6- to 12-fold lower values than for apoJ (14), consistent with the *in vitro* inhibition constants for gp330–apoJ interaction by apoE (18).

How binding of apoJ or apoJ complexes to gp330 on brain capillaries might lead to accumulation of these ligands in the vasculature and their transcytosis into the brain is unknown. It has been suggested that gp330-mediated apoJ endocytosis in several cell lines leads to lysosomal degradation (18). Our preliminary HPLC analysis of the material taken up by the brain after 10-min perfusion indicates the presence of an apparently intact apoJ, as evaluated by SDS/PAGE followed by autoradiography (Fig. 6*B*). It is possible that longer exposure times may result in some degradation of circulating apoJ in brain, but it is unlikely that gp330 would be involved in this process because the present data indicate its absence from the capillary-depleted brain (Fig. 6*A*). On the other hand we have found that $sA\beta_{1-40}$ alone is slowly degraded in brain following the BBB transport (unpublished observations). Because our *in vitro* studies have demonstrated that complexing to apoJ protects $sA\beta_{1-40}$ and $sA\beta_{1-42}$ from proteolytic degradation (unpublished observations), it is conceivable that apoJ may have similar effects on $sA\beta$ *in vivo*. Whether the $sA\beta$ is released from the complex following $sA\beta_{1-40}$–apoJ BBB uptake should be investigated. In addition to undergoing endocytosis, some of the ectodomain of gp330/megalin can be shed following combination with ligands or surrogate ligands (antibodies), either as the result of proteolytic cleavage or release of a form lacking a transmembrane and cytoplasmic domain (25). It is not known whether any shedding of gp330 occurs from cerebral endothelial cells. At present it is also unknown whether the mutated form of $A\beta_{1-40}$ found in the Dutch family (for review, see ref. 1) has different affinity to apoJ, and whether different transport properties at the BBB may lead to progressive accumulation of cerebrovascular amyloid. Answers to these questions should lead to a better understanding the role of gp330/megalin-mediated $sA\beta_{1-40}$–apoJ transport within the central nervous system, its physiological importance, and its relationship to Alzheimer disease and related disorders.

The work was supported by National Institutes of Health Grants NS34467, AG10953 (Leadership and Excellence in Alzheimer's Disease), and DK4630.

1. Wisniewski, T., Ghiso, J. & Frangione, B. (1994) *Neurobiol. Aging* **15,** 143–152.
2. Shoji, M., Golde, T., Ghiso, J., Cheung, T., Estus, S., Shaffer, L., Cai, X.-D., McKay, D., Tintner, R., Frangione, B. & Younkin, S. (1992) *Science* **258,** 126–129.
3. Haass, C., Schlossmacher, M., Hung, A., Vigo-Pelfrey, C., Mellon, A., Ostaszewski, B., Lieberburg, I., Koo, E., Schenk, D., Teplow, D. & Selkoe, D. J. (1992) *Nature (London)* **359,** 322–326.
4. Seubert, P., Vigo-Pelfrey, C., Esch, F., Lee, M., Dovey, H., Davis, D., Sinha, S., Schlossmacher, M., Whaley, J., Swindlehurst, C., McCormack, R., Wolfert, R., Selkoe, D., Lieberburg, I. & Schenk, D. (1992) *Nature (London)* **359,** 325–327.
5. Zlokovic, B. V., Ghiso, J., Mackic, J. B., McComb, J. G., Weiss, M. H. & Frangione, B. (1993) *Biochem. Biophys. Res. Commun.* **197,** 1034–1040.
6. Maness, L. M., Banks, W., Podlisny, M. B., Selkoe, D. J. & Kastin, A. (1994) *Life Sci.* **58,** 1643–1650.
7. Ghiso, J., Wisniewski, T. & Frangione, B. (1994) *Mol. Neurobiol.* **8,** 49–64.
8. Jenne, D. E. & Tschopp, J. (1992) *Trends Biochem. Sci.* **17,** 154–159.
9. Oda T., Wals, P., Osterburg, H. H., Johnson, S. A., Pasinetti, G. M., Morgan, T. E., Rozovsky I., Stine, W. B., Snyder, S. W., Holzman, T. F., Krafft, G. A. & Finch, C. E. (1995) *Exp. Neurol.* **136,** 22–31.
10. Ghiso, J., Matsubara, E., Koudinov, A., Choi-Miura, N. H., Tomita, M., Wisniewski, T. & Frangione, B. (1993) *Biochem. J.* **293,** 27–30.
11. Strittmatter, W., Saunders, A., Schmechel, D., Pericak-Vance, M., Enghild, J., Salversen, G. & Roses, A. (1993) *Proc. Natl. Acad. Sci. USA* **90,** 1977–1981.
12. Matsubara, E., Frangione B. & Ghiso, J. (1995) *J. Biol. Chem.* **270,** 7563–7567.
13. Zlokovic, B. V. (1990) *J. Controlled Release* **13,** 185–202.
14. Zlokovic B. V. (1995) *Pharmacol. Res.* **12,** 1395–1406.
15. Zlokovic, B. V., Martel, C., Mackic, J. B., Matsubara, E., Wisniewski, T., McComb, J. G., Frangione, B. & Ghiso, J. (1994) *Biochem. Biophys. Res. Commun.* **205,** 1431–1437.
16. Saito, A., Pietromonaco, S., Loo, A. K.-C. & Farquhar, M. G. (1994) *Proc. Natl. Acad. Sci. USA* **91,** 9725–9729.
17. Raychowdhury, R., Niles, J. L., McCluskey, R. T. & Smith, J. A. (1989) *Science* **244,** 1163–1165.
18. Kounnas, M. Z., Loukinova, E. B., Stefansson, S., Harmony, J. A. K., Brewer, B. H., Strickland, D. K. & Argraves, W. S. (1995) *J. Biol. Chem.* **270,** 13070–13075.
19. Farquhar, M. G., Saito, A., Kerjaschki, D. & Orlando, R. A. (1995) *J. Am. Soc. Nephrol.* **6,** 35–47.
20. Abbate, M., Bachinsky, D., Zheng, G., Stamenkovic, I., McLaughlin, M. Niles, J. L., McCluskey, R. T. & Brown, D. (1993) *Eur. J. Cell Biol.* **61,** 139–149.
21. Willnow, T. E., Goldstein, J. L., Orth, K. Brown, M. S. & Herz, J. (1992) *J. Biol. Chem.* **267,** 26172–26180.
22. Farquhar, M. G. (1995) *J. Clin. Invest.* **96,** 1184.
23. Moestrup, S. K., Cui, S., Vorum, H., Bregengard, C., Bjorn, S. E., Norris, K., Glieman, J. & Christensen, E. I. (1995) *J. Clin. Invest.* **96,** 1404–1413.
24. Saito, Y., Buciak, J., Yang, J. & Pardridge, W. M. (1995) *Proc. Natl. Acad. Sci. USA* **92,** 10227–10231.
25. Bachinsky, D. R., Zheng, G., Niles, J. L., McLaughlin, M., Abbate, M., Andres, G., Brown, D. & McCluskey, R. T. (1993) *Am. J. Pathol.* **143,** 598–611.
26. Zheng, G., Bachinsky, D. R., Stamenkovic, I., Strickland, D. K., Brown, D., Andres, G. & McCluskey, R. T. (1994) *J. Histochem. Cytochem.* **42,** 531–542.
27. Kounnas, M. Z., Chappell, D. A., Strickland, D. K. & Argaves, W. S. (1993) *J. Biol. Chem.* **268,** 14176–14181.
28. Herz, J., Goldstein, J. L., Strickland, D. K., Ho, Y. K. & Brown, M. S. (1991) *J. Biol. Chem.* **266,** 21232–21238.
29. Zlokovic, B. V., Mackic, J. B., Wang, L., McComb, J. G. & McDonough, A. A. (1993) *J. Biol. Chem.* **268,** 8019–8025.
30. Poduslo, J. F., Curran, G. L. & Berg, C. (1994) *Proc. Natl. Acad. Sci. USA* **91,** 5705–5709.
31. Pardridge, W. M. (1995) *Pharmacol. Res.* **12,** 807–816.
32. Koudinov, A., Matsubara, E., Frangione, B. & Ghiso, J. (1994) *Biochem. Biophys. Res. Commun.* **205,** 1164–1171.
33. de Silva, H. V., Stuart, W. D., Duvic, C. R., Wetterau, J. R., Ray, M. J., Ferguson, D. G., Albers, H. W., Smith, W. R. & Harmony, J. A. K. (1990) *J. Biol. Chem.* **265,** 13240–13247.
34. Glass, C. K., Pittman, R. C., Keller, G. A. & Steinberg, D. (1983) *J. Biol. Chem.* **258,** 7161–7167.
35. Moestrup, S. K., Nielsen, S., Andreasen, P., Jorgensen, K. E., Nykjaer, A., Roigaard, H., Gliemann, J. & Christensen, E. I. (1993) *J. Biol. Chem.* **268,** 16564–16570.
36. Kounnas, M. Z., Haudenschild, C. C., Strickland, D. K. & Argraves, S. W. (1994) *In Vivo* **8,** 434–352.
37. Kerjaschki, D. & Farquhar, M. G. (1983) *J. Exp. Med.* **157,** 667–686.
38. Kerjaschki, D., Horvat, R., Binder, S., Susani, M., Dekan, G., Ojha, P. P., Hillemanns, P., Ulrich, W. & Donini, U. (1987) *Am. J. Pathol.* **129,** 183–191.
39. Matsuo, S., Fukatsu, A., Taub, M. L., Caldwell, P. R. B., Brentjens, J. R. & Andres, G. (1987) *Clin. Invest.* **79,** 1798–1811.
40. Schlosshauer, B. (1993) *BioEssays* **15,** 341–346.
41. Kerjaschki, D., Miettinen, A. & Farquhar, M. G. (1987) *J. Exp. Med.* **166,** 109–128.
42. Willnow, T. E., Sheng, Z., Ishibashi, S. & Herz, J. (1994) *Science* **264,** 1471–1474.